# Low-Reynolds-number translation of a slender cylinder near a plane wall*

N. J. DE MESTRE

*Mathematics Department, Royal Military College, Duntroon, Australia*

W. B. RUSSEL

*Department of Applied Mathematics and Theoretical Physics, University of Cambridge, Cambridge, England*

(Received March 6, 1974 and in final form August 12, 1974)

SUMMARY

Low-Reynolds-number results are presented for the drag and induced torque on a slender circular cylinder translating near a single plane wall. Four representative situations are investigated, the principal feature of the analysis being that it is valid for all distances from the wall which are large compared with the radius of the cylinder. In particular, the results hold for distances from the wall of the same order of magnitude as the length of the cylinder. The direction and rate of rotation are given for those cases where it occurs.

## 1. Introduction

Low-Reynolds-number slender-body theory has applications in several fields of fluid flow. In suspension mechanics it predicts both the bulk stresses and sedimentation rates of dispersions of long fibres in a Newtonian liquid. The earliest application, however, was in biomechanics, where Hancock [1] used the theory to investigate the self-propulsion of microscopic organisms by flagella, while Blake [2] has recently applied it to ciliary propulsion.

In both these fields situations are encountered where the fibres or organisms interact significantly with solid boundaries. These occur, for example, in micro-organism motion between a microscope slide and coverslip, in ciliated micro-organisms since the slender organelles beat near the cell surface, and in the flow of suspensions during processing. Although wall effects are thus sometimes important at low Reynolds numbers, only a few papers have considered the problem.

In each of these a slender body translating near a wall is approximated by a distribution of point forces, called Stokeslets, along the body axis and an image system in the wall. The strengths of these forces are then determined such that the no-slip conditions are satisfied on both surfaces. Takaisi [3] applied an approximate technique developed by Burgers [4] to obtain a polynomial expression for the Stokeslet strengths, while Blake [5] solved the appropriate integral equations numerically and obtained the extra drag on the body due to the wall. De Mestre [6] obtained analytic solutions for the special cases of a circular cylinder (i) moving parallel to a plane surface but normal to its own axis and (ii) moving parallel to and midway between two walls. Related experiments supported the predictions. Experimental and theoretical results could not be compared for any other orientations of the cylinder near the plane surface because fixed orientations could not be maintained during an experimental run. The cylinder rotated and drifted away from the wall as soon as it was released, even for the case of axial fall.

In this paper we extend the technique used in de Mestre [6] to present analytical results for two of these rotating-rod situations, namely the representative orientations of axial fall parallel to a plane vertical wall and transverse fall in a vertical plane normal to the vertical wall. In addition, the related cases of axial and transverse fall towards a horizontal wall are treated.

For each of these four configurations the drag in the far-field limit agrees with that obtained from Brenner's [7] solution for a body of arbitrary shape falling far from a single plane wall. Likewise, for orientations parallel to the wall, a near-wall asymptotic expansion of the predicted Stokeslet strength leads to the expressions given recently by Lighthill [8]. The complete solutions thus provide continuity between two known limiting cases.

## 2. Slender body analysis

The hydrodynamic disturbance caused by the low-Reynolds-number rotation or translation of a slender body can be represented by a distribution of singularities along its axis, a well-known method which can be formulated either intuitively or from a surface integral solution to the Stokes equations. We will not dwell on such developments here, but will proceed directly to the added effect of a nearby solid boundary. A second system of singularities must then be distributed along the axis of the slender body's image in the wall in order to produce zero velocity on the additional surface.

The number of types of singularities which must be placed within a body to describe exactly the distributed flow field outside depends on both the symmetry of the body and the flow. When the body is slender, the total drag and torque can be obtained to a useful order of approximation by considering only a distribution of point forces (Stokeslets) over a line enclosed by the body. The image system for a point force $F_j$ at a distance $h$ from a plane wall has been determined by Blake [9] and consists of a Stokeslet of equal magnitude but opposite sign plus a Stokes-doublet of strength $2hF_j$ and a source-doublet of strength $2h^2F_j$. Incorporation of these into the Stokeslet representation for a slender body in the absence of the wall gives the induced velocity at any point of the fluid when there is no-slip on the plane wall.

For each of the four cases under consideration we use a rectangular co-ordinate system which moves with the rod. Suppose $x_3 = 0$ represents the wall and that the axis of the rod lies in the $x_1 x_3$-plane at different orientations depending on the case considered but such that the centre of mass has co-ordinates $(0, 0, L)$.

If $y_i$ denotes the co-ordinates of a point on the axis of the rod of length $2l$, $Y_i$ the co-ordinates of the corresponding image point in the wall, $s$ the directed distance from the centre of mass along the body's axis, and $\mu$ denotes the dynamic viscosity, the induced velocity due the Stokeslets and their images has the form

$$
u_i(x) = \frac{1}{8\pi\mu} \int_{-l}^{+l} F_j(s) \left\{ \left( \frac{1}{r} - \frac{1}{R} \right) \delta_{ij} + \frac{r_i r_j}{r^3} - \frac{R_i R_j}{R^3} \right.
$$

$$
\left. + 2h(s)(\delta_{j\alpha}\delta_{k\alpha} - \delta_{j3}\delta_{k3}) \frac{\partial}{\partial R_k} \left( \frac{h(s)R_i}{R^3} - \frac{\delta_{i3}}{R} - \frac{R_i R_3}{R^3} \right) \right\} ds \tag{1}
$$

where $\alpha = 1, 2$ only; $i, j$ and $k = 1, 2$ or $3$; $r_i = x_i - y_i$, $r^2 = r_i r_i$, $R_i = x_i - Y_i$ and $R^2 = R_i R_i$. The terms containing $r$ refer to the Stokeslet distribution inside the body, while those containing $R$ arise from the image system and thus represent the effect of the plane wall boundary on the flow.

To solve a particular problem one must choose $F_j(s)$ such that the desired velocity field (rigid body rotation or translation) is produced at the surface of the body. For a slender rod in the shape of a circular cylinder of radius $R_0$ and length $2l$, both $R_0/l$ and the parameter

$$
\varepsilon = \{\ln(2l/R_0)\}^{-1}
$$

are small; thus, the integrals can be expanded asymptotically and the $F_j$ easily determined. The theory to be developed is valid for $R_0 \ll l$ and $L$, but there is no restriction on the relative magnitudes of $l$ and $L$.

### 2.1. CASE I

For axial motion of the cylinder parallel to the boundary as shown in Fig. 1 we have

$$
s = x_1, \quad y_i = x_1 \delta_{i1} + L\delta_{i3}, \quad Y_i = x_1 \delta_{i1} - L\delta_{i3}, \quad h = L .
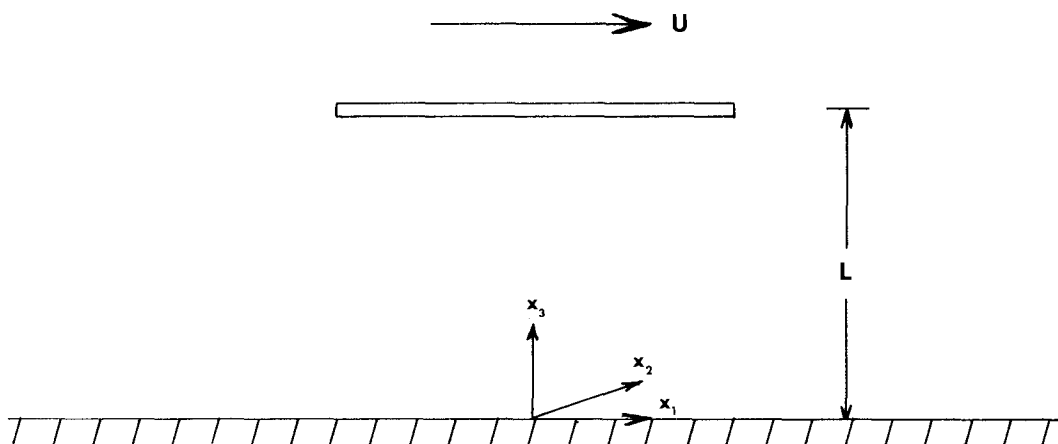$$

Figure 1

When a rod moves axially in an unbounded fluid the flow field can be approximated by Stokeslets solely in the axial direction. However, the problem for axial motion parallel to a wall requires that Stokeslets normal to the wall be included also. The condition for zero slip on the surface $x_i = (x_1, R_0 \cos \phi, L + R_0 \sin \phi)$ of the rod is then formulated from Eqn. (1) as

$$
U_i = \frac{1}{8\pi\mu} \int_{-l}^{+l} F_1(s) \left\{ \left( \frac{1}{r} - \frac{1}{R} \right) \delta_{i1} + \frac{r_i r_1}{r^3} - \frac{R_i R_1}{R^3} + 2L\delta_{k1} \frac{\partial}{\partial R_k} \left( \frac{LR_i}{R^3} - \frac{\delta_{i3}}{R} - \frac{R_i R_3}{R^3} \right) \right\} ds
$$

$$
+ \frac{1}{8\pi\mu} \int_{-l}^{+l} F_3(s) \left\{ \left( \frac{1}{r} - \frac{1}{R} \right) \delta_{i3} + \frac{r_i r_3}{r^3} - \frac{R_i R_3}{R^3} - 2L\delta_{k3} \frac{\partial}{\partial R_k} \left( \frac{LR_i}{R^3} - \frac{\delta_{i3}}{R} - \frac{R_i R_3}{R^3} \right) \right\} ds
$$

$$(2)$$

where $r_i = (x_1 - s, R_0 \cos \phi, R_0 \sin \phi)$, $R_i = (x_1 - s, R_0 \cos \phi, 2L + R_0 \sin \phi)$ and for a rod with translational speed $U$ and angular speed $\omega$ about the $x_2$ axis $U_i = (U, 0, \omega x_1)$.

For $R_0/l$ and $R_0/L$ both small an asymptotic expansion of the integrals in Eqn. (2) as suggested by Batchelor [10] yields

$$
U = \frac{F_1(x_1)}{8\pi\mu} \left\{ 4 \ln \left( \frac{2l}{R_0} \right) + 2 \ln \left( 1 - \frac{x_1^2}{l^2} \right) - 2 - E_1(x_1) + O \left( \frac{R_0}{l}, \frac{R_0}{L} \right) \right\}
$$

$$
+ \frac{1}{8\pi\mu} \int_{-l}^{+l} \{F_1(s) - F_1(x_1)\} H_1(x_1, s) ds - \frac{L^3}{\pi\mu} F_3(x_1) G(x_1) + O \left( \frac{R_0}{l} F_3 \right), \qquad (3)
$$

$$
0 = O \left( \frac{R_0}{l} F_1, \frac{R_0}{l} F_3 \right), \qquad (4)
$$

$$
\omega x_1 = \frac{L^3}{\pi\mu} F_1(x_1) G(x_1) + \frac{F_3(x_1)}{4\pi\mu\varepsilon} + O \left( \frac{R_0}{l} F_1, F_3 \right), \qquad (5)
$$

where

$$
G(x_1) = \frac{1}{\{(l - x_1)^2 + 4L^2\}^{\frac{3}{2}}} - \frac{1}{\{(l + x_1)^2 + 4L^2\}^{\frac{3}{2}}},
$$

$$
H_1(x_1, s) = \frac{2}{|x_1 - s|} - \frac{2}{\rho} + \frac{2L^2}{\rho^3} + \frac{6L^2(x_1 - s)^2}{\rho^5} \quad \text{with} \quad \rho^2 = (x_1 - s)^2 + 4L^2,
$$

$$E_I(x_1) = 2 \operatorname{arcsinh}\left(\frac{l+x_1}{2L}\right) + 2 \operatorname{arcsinh}\left(\frac{l-x_1}{2L}\right) + \frac{(l+x_1)}{\{(l+x_1)^2 + 4L^2\}^{\frac{1}{2}}}$$

$$+ \frac{(l-x_1)}{\{(l-x_1)^2 + 4L^2\}^{\frac{1}{2}}} - \frac{2L^2(l+x_1)}{\{(l+x_1)^2 + 4L^2\}^{\frac{3}{2}}} - \frac{2L^2(l-x_1)}{\{(l-x_1)^2 + 4L^2\}^{\frac{3}{2}}} \,.$$

Equations (3)–(5) are satisfied to order $\varepsilon^2$ by choosing

$$F_1 = \frac{8\pi\mu U\varepsilon}{4 + \varepsilon\left\{2\ln\left(1 - \frac{x_1^2}{l^2}\right) - 2 - E_I\right\}} + O(\varepsilon^3), \tag{6}$$

$$F_3 = 4\pi\mu\varepsilon\{\omega_{x1} - 2\varepsilon U L^3 G(x_1)\} + O(\varepsilon^3), \tag{7}$$

where $\omega$ is $O(\varepsilon)$ as will be shown shortly. The $\varepsilon$-term must be retained in the denominator of Eqn. (6) because $E_I$ becomes large as $L/l \to 0$.

Now the total drag on the rod is given by

$$\mathscr{F}_1 = \int_{-l}^{+l} F_1(x_1)dx_1 \,,$$

and to the order considered in Eqn. (7) it is seen that the net lateral force

$$\int_{-l}^{+l} F_3(x_1)dx_1 = 0 \,.$$

Thus, provided $\varepsilon E_I$ is $o(1)$ as $\varepsilon \to 0$ the total drag is obtained from Eqn. (6) as

$$\mathscr{F}_1 = 2\pi\mu U\varepsilon l\left[2 + \varepsilon\{-0.614 + W_1\} + O\left(\varepsilon^2, \frac{\varepsilon R_0}{L}\right)\right]$$

where

$$W_1 = 2\operatorname{arcsinh}\frac{l}{L} - 3\left(1 + \frac{L^2}{l^2}\right)^{\frac{1}{2}} + \frac{7L}{2l} - \frac{L^2}{2l^2\left(1 + \frac{L^2}{l^2}\right)^{\frac{1}{2}}}$$

is the contribution due to the presence of the wall. For closer approaches to the wall an expansion in $L/l$ or a straight numerical integration of Eqn. (6) must be performed.

The limiting forms of this drag expression are
(i) the far-field solution which $l/L \to 0$ and

$$\mathscr{F}_1 = 2\pi\mu U\varepsilon l\left[2 + \varepsilon\left\{-0.614 + \frac{3l}{4L}\right\} + O\left(\varepsilon\frac{l^3}{L^3}, \varepsilon^3\right)\right],$$

a particular case of Brenner's [7] more general result for arbitrary-shaped bodies, and
(ii) the near-field solution for which $l \gg L \gg R_0$ and hence letting $L/l \to 0$ in Eqn. (6) yields

$$\mathscr{F}_1 \approx \frac{4\pi\mu Ul}{\ln(2L/R_0)},$$

agreeing with the results given by Lighthill [8].

The angular velocity of the rod is calculated from the fact that there is no resultant torque on it in this pseudo-steady situation. Now the Stokeslets $F_1$ produce zero moment about the centre of mass of the rod, therefore

$$\int_{-l}^{+l} x_1 F_3(x_1)dx_1 = 0$$

which yields from Eqn. (7)

$$\omega = \varepsilon 3U(L/l)^3 \int_{-l}^{+l} x_1 G(x_1)dx_1 + O(\varepsilon^2)$$

$$= \frac{\varepsilon 3UL^2}{l^3}\left\{\frac{1 + l^2/(2L^2)}{(1 + l^2/L^2)^{\frac{1}{2}}} - 1\right\} + O(\varepsilon^2)$$

as $\varepsilon \to 0$. It is interesting to note that for fixed $U$ and $l$ the angular speed is a maximum at $L \approx 0.45l$. Since the dominant term in the expansion for $\omega$ is positive, the rod rotates so that its leading end moves away from the wall, an effect which has been observed experimentally by de Mestre [6].

If the rod is prevented from rotating by an applied external couple then $\omega = 0$ in Eqn. (5) and hence in Eqn. (7). Thus the required couple $\mathscr{L}_i$ has components

$$\mathscr{L}_1 = \mathscr{L}_3 = 0, \quad \mathscr{L}_2 = \varepsilon^2 \, 8\pi\mu U L^2 \left\{ 1 - \frac{1 + l^2/(2L^2)}{(1 + l^2/L^2)^{\frac{1}{2}}} \right\}.$$

## 2.2. CASE II

For a cylinder parallel to the wall and approaching it with velocity $U$ as shown in Fig. 2 the co-ordinates of Case I are still appropriate. Besides employing distributions of Stokeslets in the $x_1$ and $x_3$ directions this problem is conveniently solved by including an axial distribution of source-doublets in the $x_3$ direction with the appropriate image system.

The image system for a source-doublet of strength $D_j$ at a distance $h$ from a plane wall $x_3 = 0$ can be obtained from Lorentz [11]. The corresponding velocity field is

$$u_i(x) = \frac{D_j}{8\pi\mu} \left\{ -\frac{\delta_{ij}}{r^3} + \frac{3r_i r_j}{r^5} + (\delta_{i3}\delta_{3k} - \delta_{i\alpha}\delta_{\alpha k})\left(\frac{\delta_{jk}}{R^3} - \frac{3R_j R_k}{R^5}\right) - 2h\frac{\partial}{\partial R_i}\left(\frac{\delta_{3j}}{R^3} - \frac{3R_3 R_j}{R^5}\right)\right\}$$

with all variables defined as for Eqn. (1). Thus the no-slip condition on the rod for this case is

$$V_i = \frac{1}{8\pi\mu}\int_{-l}^{+l} F_1(s) \left\{\left(\frac{1}{r} - \frac{1}{R}\right)\delta_{i1} + \frac{r_i r_1}{r^3} - \frac{R_i R_1}{R^3} + L\delta_{k1}\frac{\partial}{\partial R_k}\left(\frac{LR_i}{R^3} - \frac{\delta_{i3}}{R} - \frac{R_i R_3}{R^3}\right)\right\} \, ds$$

$$+ \frac{1}{8\pi\mu}\int_{-l}^{+l} F_3(s) \left\{\left(\frac{1}{r} - \frac{1}{R}\right)\delta_{i3} + \frac{r_i r_3}{r^3} - \frac{R_i R_3}{R^3} - L\delta_{k3}\frac{\partial}{\partial R_k}\left(\frac{LR_i}{R^3} - \frac{\delta_{i3}}{R} - \frac{R_i R_3}{R^3}\right)\right\} \, ds$$

$$+ \frac{1}{8\pi\mu}\int_{-l}^{+l} D_3(s) \left\{-\frac{\delta_{i3}}{r^3} + \frac{3r_i r_3}{r^5} + (\delta_{i3}\delta_{3k} - \delta_{i\alpha}\delta_{\alpha k})\left(\frac{\delta_{3k}}{R^3} - \frac{3R_3 R_k}{R^5}\right)\right.$$

$$\left. - 2L\frac{\partial}{\partial R_i}\left(\frac{1}{R^3} - \frac{3R_3^2}{R^5}\right)\right\} ds \quad (8)$$
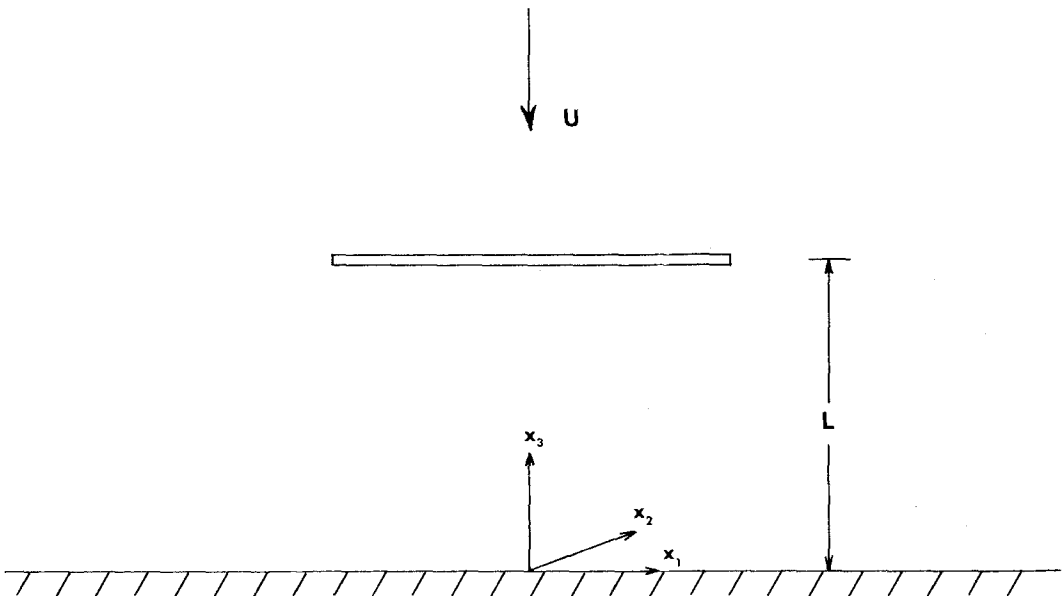
Figure 2

where symmetry of the flow about the $x_3$ axis means that $V_i = (0, 0, -U)$.

The slender-body expansion of Eqn. (8) for $R_0/l$ and $R_0/L$ both small is similar to Case I and yields

$$0 = \frac{F_1(x_1)}{2\pi\mu\varepsilon} - \frac{L^3}{\pi\mu} F_3(x_1) G(x_1) + O\left(F_1, \frac{R_0}{l} F_3, \frac{D_3}{l^2}\right)$$

$$0 = O\left(\frac{R_0}{l} F_1, \frac{R_0}{l} F_3, \frac{R_0}{l^3} D_3\right)$$

$$-U = \frac{L^3}{\pi\mu} F_1(x_1) G(x_1) + O\left(\frac{R_0}{l} F_1\right)$$

$$+ \frac{F_3(x_1)}{8\pi\mu} \left\{2 \ln\left(\frac{2l}{R_0}\right) + \ln\left(1 - \frac{x_1^2}{l^2}\right) + 2\cos^2\phi - E_{\text{II}} + O\left(\frac{R_0}{l}, \frac{R_0}{L}\right)\right\}$$

$$+ \frac{1}{8\pi\mu} \int_{-l}^{+l} \{F_3(s) - F_3(x_1)\} H_{\text{II}}(x_1, s) ds$$

$$+ \frac{D_3}{8\pi\mu} \left\{-\frac{2}{R_0^2} + \frac{4\cos^2\phi}{R_0^2} + O(1)\right\} \tag{9}$$

where

$$H_{\text{II}}(x_1, s) = \frac{1}{|x_1 - s|} - \frac{1}{\rho} - \frac{2L^2}{\rho^3} - \frac{24L^4}{\rho^5}$$

and

$$E_{\text{II}} = \text{arcsinh}\left(\frac{l+x_1}{2L}\right) + \text{arcsinh}\left(\frac{l-x_1}{2L}\right) + \frac{2(l+x_1)}{\{(l+x_1)^2 + 4L^2\}^{\frac{1}{2}}}$$

$$+ \frac{2(l-x_1)}{\{(l-x_1)^2 + 4L^2\}^{\frac{1}{2}}} - \frac{(l+x_1)^3}{2\{(l+x_1)^2 + 4L^2\}^{\frac{3}{2}}} - \frac{(l-x_1)^3}{2\{(l-x_1)^2 + 4L^2\}^{\frac{3}{2}}}.$$

In a similar manner to Hancock [1] we remove the $\phi$-dependence in Eqn. (9) by choosing

$$D_3(x_1) = -\tfrac{1}{2} R_0^2 F_3(x_1)$$

and then the asymptotic solutions for the Stokeslet strengths are

$$F_3(x_1) = \frac{-8\pi\mu U\varepsilon}{2 + \varepsilon\left\{\ln\left(1 - \frac{x_1^2}{l^2}\right) + 1 - E_{\text{II}}\right\}} + O(\varepsilon^3) \tag{10}$$

and

$$F_1(x_1) = -\varepsilon^2 4\pi\mu U L^3 G(x_1).$$

The symmetry of the Stokeslet strengths about the $x_3$ axis means that there is no rotation in this case.

Since $F_1$ is an odd function of $x_1$ the total drag on the cylinder is

$$\mathscr{F}_{\text{II}} = \int_{-l}^{+l} F_3(x_1) dx_1$$
$$= -4\pi\mu U\varepsilon l[2 + \varepsilon\{-1.386 + W_{\text{II}}\} + O(\varepsilon^2, \varepsilon R_0/L)]$$

when the wall effect

$$W_{\text{II}} = 2 \, \text{arcsinh} \frac{l}{L} + \frac{1}{(1 + L^2/l^2)^{\frac{1}{2}}}$$

is $O(1)$, but for closer approaches the total drag must be calculated either numerically or by expanding Eqn. (10) for $L/l \ll 1$.

As $l/L \to 0$ the far-field limit

$$\mathscr{F}_{\text{II}} = -4\pi\mu U\varepsilon l\left[2+\varepsilon\left\{-1.386+\frac{3l}{L}\right\}+O\left(\varepsilon\frac{l^3}{L^3},\varepsilon^2\right)\right]$$

while as $L/l \to 0$ $(l \gg L \gg R_0)$ the near-field limit becomes

$$\mathscr{F}_{\text{II}} \approx \frac{-8\pi\mu Ul}{\ln(2L/R_0)-1}.$$

These agree respectively with the results given by Brenner [7] and Lighthill [8].

*2.3. CASE III*

For the cylinder in Fig. 3 which is oriented normal to the wall but is moving with velocity $U$ parallel to it, the co-ordinates appropriate to Eqn. (1) are now

$$s = x_3 - L, \quad y_i = x_3\delta_{i3}, \quad Y_i = -x_3\delta_{i3}, \quad h = x_3 .$$

A similar analysis to Case II using a Stokeslet distribution $F_1(x_3)$ and source-doublet distribution $D_1(x_3) = -\frac{1}{2}R_0^2 F_1(x_3)$ along the axis $L-l < x_3 < L+l$, $x_1 = x_2 = 0$ of the rod yields

$$F_1(x_3) = \frac{8\pi\mu U\varepsilon}{2+\varepsilon\left[\ln\left\{1-\frac{(x_3-L)^2}{l^2}\right\}+1-E_{\text{III}}\right]} + O(\varepsilon^3)$$

and

$$\mathscr{F}_{\text{III}} = \int_{L-l}^{L+l} F_1(x_3)\,dx_3$$

$$= 4\pi\mu U\varepsilon l[2+\varepsilon\{-1.386+W_{\text{III}}\}+O(\varepsilon^2)]$$

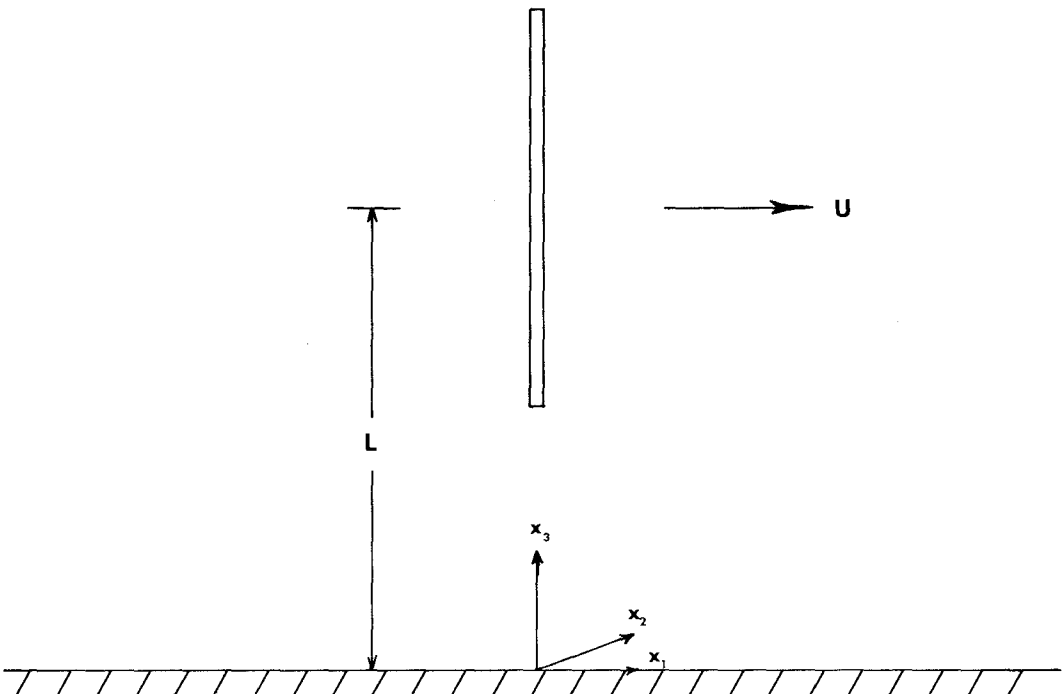where



L

U

$x_3$

$x_2$

$x_1$

Figure 3

$$E_{\text{III}} = \ln\left(\frac{x_3 + L + l}{x_3 + L - l}\right) + \frac{4lx_3(Lx_3 + L^2 - l^2)}{(x_3^2 + 2Lx_3 + L^2 - l^2)^2}$$

and

$$W_{\text{III}} = \left(\frac{L}{l} + 1\right) \ln\left(1 + \frac{l}{L}\right) + \left(\frac{L}{l} - 1\right) \ln\left(1 - \frac{l}{L}\right) + \frac{l}{2L}$$

reflect the wall influence.

While the far-field limit of $\mathscr{F}_{\text{III}}$ agrees with [7], in the limit as $L/l \to 1$ it is noted that $W_{\text{III}}$ remains finite, contradicting physical expectations. The results are no longer valid, however, when the end of the rod approaches within a few radii of the wall. Then the flow in the neighbourhood of this end, which makes a considerable contribution to the total drag, cannot be determined accurately enough by a line distribution of Stokeslets. The correct approach would be to consider a surface distribution, although in this case lubrication theory might be a more tractable alternative.

Intuitively, one would expect a couple-free rod moving as in Fig. 3 to rotate about its centre of mass since the end closer to the wall must move slower. Indeed, the couple needed to maintain the rod normal to the wall has components

$$\mathscr{L}_1 = \mathscr{L}_3 = 0,$$

$$\mathscr{L}_2 = \int_{L-l}^{L+l} (x_3 - L) F_1 \, dx_3$$

$$= -\varepsilon^2 \, 2\pi\mu U l^2 \left\{ 1 + \left(\frac{L^2}{l^2} - 1\right) \ln\left(1 - \frac{l^2}{L^2}\right) \right\} + O(\varepsilon^3).$$

Alternatively, if the rod is free to rotate, its angular velocity

$$\omega = \frac{3}{8\pi\mu l^3 \varepsilon} \mathscr{L}_2$$

is again an $O(\varepsilon)$ effect.

## 2.4. CASE IV

Finally, for a cylinder approaching the wall along its axis with velocity $U$ (Fig. 4), the co-ordinates of the last case can again be used in Eqn. (1) for a Stokeslet distribution $F_3(x_3)$ only, because the flow field is axisymmetric. The appropriate integral equations yield

$$F_3(x_3) = -\frac{4\pi\mu U\varepsilon}{2 + \varepsilon\left[\ln\left\{1 - \frac{(x_3 - L)^2}{l^2}\right\} - 1 - E_{\text{III}}\right]} + O(\varepsilon^3)$$

and

$$\mathscr{F}_{\text{IV}} = -2\pi\mu U\varepsilon l [2 + \varepsilon\{-0.614 + W_{\text{III}}\} + O(\varepsilon^2)].$$

In this orientation the angular velocity of the rod is zero, although it appears to be unstable to small angular perturbations.

## 3. Conclusions

As a measure of the wall influence on the total drag we compute for each case

$$\frac{\Delta\mathscr{F}}{\mathscr{F}_\infty} = \frac{\mathscr{F}_M - \mathscr{F}_\infty}{\mathscr{F}_\infty} \qquad (M = \text{I, II, III, IV})$$

where $\mathscr{F}_\infty$ denotes the drag in unbounded fluid for either axial or transverse motion, depending on the case under consideration. This wall-effect quantity is plotted against $L/l$ in Fig. 5 for a slender body with aspect ratio $l/R_0 = 50$ ($\varepsilon = 0.217$), a value near those frequently occurring in
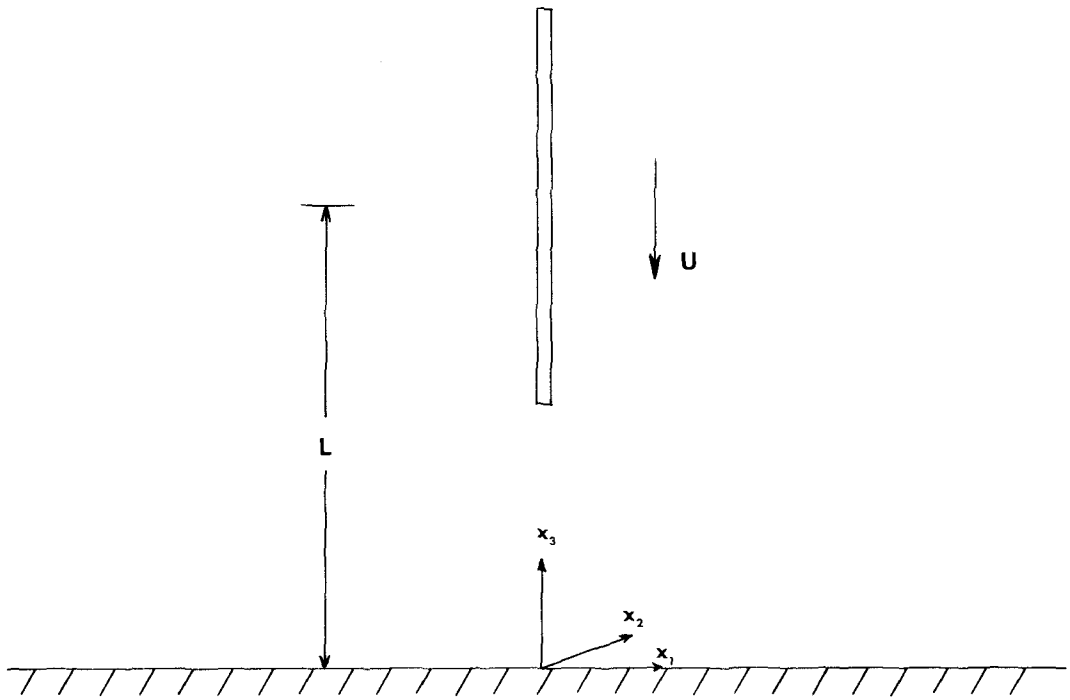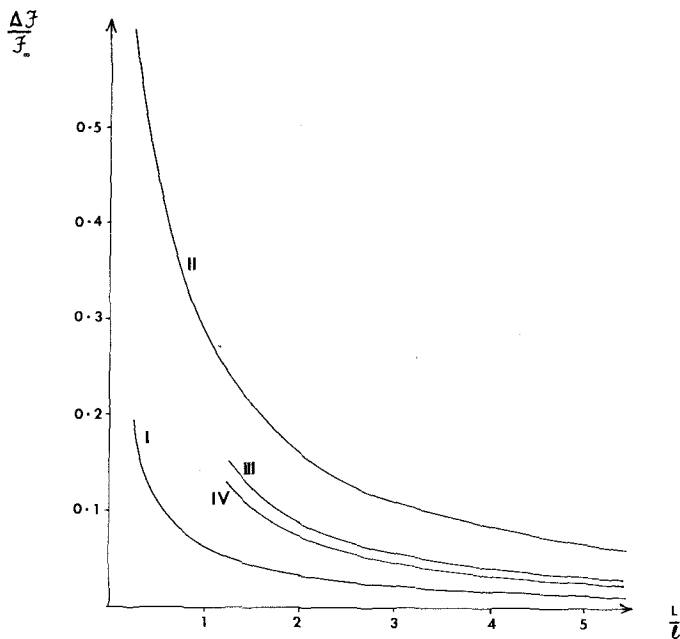
Figure 4



Figure 5

biomechanical studies. The general shapes of the curves will be the same for all slender-body values of $\varepsilon$.

Clearly the drag increases as the wall is approached. The axial motion of a rod towards or parallel to a wall (Cases IV and I) are influenced to only a small degree by the wall's presence. Transverse motion parallel to the wall (Case III) is also only slightly effected, but curve II for transverse motion towards the wall shows a sharp rise in the drag when the rod approaches within a body length.

Since Cases I and III cover extreme orientations for a rod moving parallel to a wall, it can be deduced that the wall effect is less than 15% for a rod moving parallel to a wall at any orientation when its centre of mass is more than a body length away from the wall.

For motion towards a wall it has already been suggested that Case IV covers an unstable orientation. The wall would tend to slow down the leading edge of a rod falling towards it at an angle, producing orientations that approach Case II. Thus rods falling towards a wall are appreciably slowed down as they approach within a body length of the wall.

Of course rods which are orientated neither perpendicular nor parallel to a wall move obliquely towards any wall they are approaching. The results of this paper show that it is the component of velocity normal to the wall which is influenced most of all by the wall. As a consequence of this the rod assumes a new orientation making a smaller angle with the wall. When this is combined with the rotation effect analysed in Case I it is seen that a rod approaching a vertical wall obliquely will eventually be repelled away from the wall.

It is interesting to note that outside a distance of one body length the error involved in using the approximate drag expressions obtained from Brenner [7] instead of the expressions for $\mathscr{F}_M$ given by this paper is at most 1%. Calculations show that this is true for all $\varepsilon < 0.4$ and means that Brenner's far-field expressions are in fact useful down to $L = 2l$.

The small values of $\Delta\mathscr{F}/\mathscr{F}_\infty$ for three of the curves in Fig. 5 suggest that we should consider the wall effect for distances from the wall comparable with the radius of the rod rather than its length. However the theory developed depends on $R_0/L$ being small. This means that we can only use our results to plot $\Delta\mathscr{F}/\mathscr{F}_\infty$ against $L/R_0$ values greater than 5, and this is done in Fig. 6 for the two cases of rod motion parallel to the wall (Cases I and II). For the remaining cases a more pertinent separation ratio to plot the wall effect against is $(L-l)/R_0$ (See Fig. 7). Extreme values of $\varepsilon$ were used in both figures to show the range of the effect for variations in the slender-body parameter. The upper limit of slender-body theory is taken as $2l/R_0 = 10$ ($\varepsilon =$
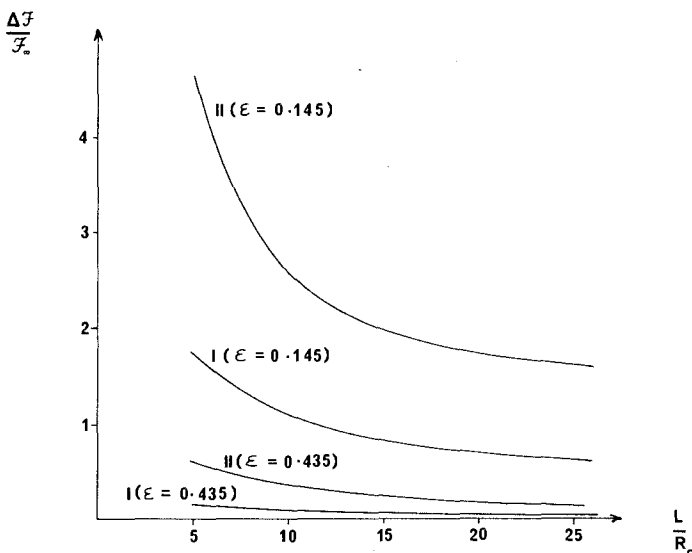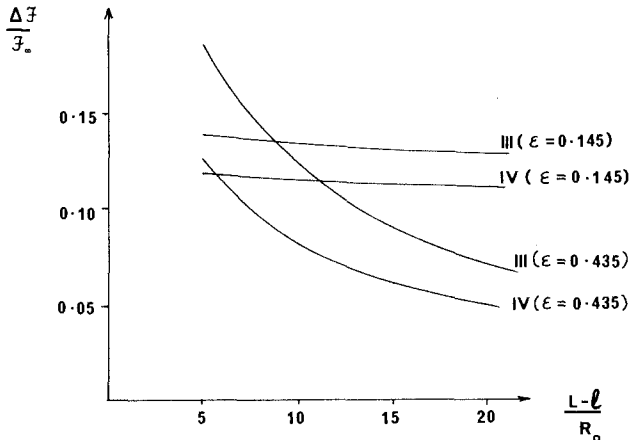


Figure 6

Figure 7.

0.435) for which the errors in using slender-body approximations are rather large. We take as an example of a very thin slender body $2l/R_0 = 1000$ ($\varepsilon = 0.145$), from which it is noted that $\varepsilon$ changes only slightly with large changes in the aspect ratio.

The curves for Case II (Fig. 6) show the dominance of the wall effect for most slender bodies in this situation once they approach within five diameters. A rod moving parallel to the wall (Case I) is not influenced as much, particularly if it is very slender. On the other hand $\Delta \mathscr{F}/\mathscr{F}_\infty$ ($M = $ III and IV) both show little variation and small magnitudes for all $\varepsilon$ as the rod approaches the wall. This emphasises the limited influence of the wall on the drag of rods normal to it.

REFERENCES

[1] G. J. Hancock, The self-propulsion of microscopic organisms through liquids, *Proc. Roy. Soc.*, A217 (1953) 96.
[2] J. R. Blake, A model for the micro-structure in ciliated organisms, *J. Fluid Mech.*, 55 (1972) 1.
[3] Y. Takaisi, *The forces on a long straight circular cylinder moving in a semi-infinite viscous liquid bounded by a plane wall.* Memoirs of the Ehime Univ. Sect II (SCI) 3, No. 1 (1958) 29.
[4] J. M. Burgers, *Second report on viscosity and plasticity*, Chapter 3, North Holland, Amsterdam (1938).
[5] J. R. Blake, Singularities of viscous flow. Part II : Applications to slender-body theory, *J. Eng. Math.*, 8 (1974) 113.
[6] N. J. de Mestre, Low-Reynolds-number fall of slender cylinders near boundaries, *J. Fluid Mech.*, 58 (1973) 641.
[7] H. Brenner, Effect of finite boundaries on the Stokes resistance of an arbitrary particle, *J. Fluid Mech.*, 12 (1962) 35.
[8] M. J. Lighthill, Mathematical Biofluiddynamics, (in press) (1974).
[9] J. R. Blake, A note on the image system for a Stokeslet in a no-slip boundary, *Proc. Camb. Phil. Soc.*, 70 (1971) 303.
[10] G. K. Batchelor, Slender-body theory for particles of arbitrary cross-section in Stokes flow, *J. Fluid Mech.*, 44 (1970) 419.
[11] H. A. Lorentz, A general theorem concerning the motion of a viscous fluid and a few consequences derived from it, *Abhandl. theoret. Phys.*, 1 (1907) 23.